

Fermi National Accelerator Laboratory

FERMILAB-Pub-93/139-E

CDF

B Physics at CDF: Results and Prospects

Michelangelo L. Mangano
for the CDF Collaboration

*Fermi National Accelerator Laboratory
P.O. Box 500, Batavia, Illinois 60510*

June 1993

To appear in *Nuclear Instruments and Methods*

Disclaimer

This report was prepared as an account of work sponsored by an agency of the United States Government. Neither the United States Government nor any agency thereof, nor any of their employees, makes any warranty, express or implied, or assumes any legal liability or responsibility for the accuracy, completeness, or usefulness of any information, apparatus, product, or process disclosed, or represents that its use would not infringe privately owned rights. Reference herein to any specific commercial product, process, or service by trade name, trademark, manufacturer, or otherwise, does not necessarily constitute or imply its endorsement, recommendation, or favoring by the United States Government or any agency thereof. The views and opinions of authors expressed herein do not necessarily state or reflect those of the United States Government or any agency thereof.

B PHYSICS AT CDF: RESULTS AND PROSPECTS ¹

FERMILAB-PUB-93/139-E

Michelangelo L. MANGANO ²
for the CDF Collaboration

In this presentation we will review the latest B physics results from the CDF Collaboration at the Fermilab Tevatron Collider. We will cover recently completed analyses of the 1988–89 data, and will describe the first preliminary results of the studies of the new 1992–93 run.

In tune with the emphasis of this Workshop, we will try to put all of these results in perspective. With the latest upgrades of the detector, CDF has today a unique opportunity to carry out important measurements of B physics and to pave the way towards the realization of more specialized detectors which will explore CP violation in the B system [1] later in the decade. Several of the unknowns in the evaluation of CP reach for the experimental proposals presented at this Workshop can be pinned down within the next few years by CDF. We will try to indicate how this will happen.

Section 1 summarizes the main detector features relevant for B identification and B -related studies. In Section 2 we will cover the studies of production mechanisms for heavy quarks. Section 3 presents the study of J/ψ and other charmonium states. Section 4 covers the measurement of the inclusive B lifetime using the J/ψ decay modes. Section 5 describes the detection of exclusive decay modes of B mesons. Section 6 contains our conclusions.

1 The CDF Detector and B Identification

The CDF detector is described in detail elsewhere [2]. Here we will limit ourselves to presenting the main components needed for B studies.

Several different channels allow the detection of bottom particles: fully reconstructed decays, high- p_t leptons from inclusive semileptonic decays, lepton pairs either from sequential b decays or from decays of both b and \bar{b} , inclusive J/ψ and ψ' mesons detected via their $\mu^+\mu^-$ and $\psi\pi\pi$ decay modes.

Muons, which are a fundamental element in most of these channels, are identified by four layers of drift chambers surrounding the central hadronic calorimeter. The coverage in pseudorapidity ($\eta = -\ln[\tan(\theta/2)]$) was extended in 1992 to $|\eta| < 1$ from the old $|\eta| < 0.63$ region. In this most central section, 0.6m of steel and a new set of drift chambers have also been added, reducing the punch through background by a factor of 5. Stubs in the muon chambers are then matched to tracks reconstructed in the central tracking chamber (CTC). The 84 layers of the CTC are immersed in a 1.4T field, which provides a momentum resolution of $\delta p_t/p_t \approx 0.0011p_t \oplus 0.006$ for central ($|\eta| < 1.2$) and

¹To appear in Nucl. Instr. and Meth., Proceedings of the 1993 UNK B-Factory Workshop, Liblice Castle, Czech Republic, 18-22 January 1993.

²Istituto Nazionale di Fisica Nucleare, Scuola Normale Superiore and Dipartimento di Fisica dell'Univerita', Pisa, ITALY. Bitnet: MLM@FNALD.FNAL.GOV

vertex-constrained charged tracks. Immediately surrounding the beam pipe is a 4-layer, single-sided silicon vertex detector (SVX), providing a resolution in the transverse position of primary and secondary vertices which is unprecedented in hadronic collisions. The primary vertex (PV) resolution in a typical event is $35\mu\text{m}$, similar to the transverse beam size. For events with higher multiplicity, such as $t\bar{t}$ events, the expected (PV) resolution is about $12\mu\text{m}$. One can use the event-by-event or run-average (PV), depending on the data sample or event topology, in order to get the best resolution and minimize the systematic errors. The impact parameter resolution for tracks hitting all 4 layers of the SVX can be parameterized, as a function of p_t , as follows: $\sigma_{IP} = a/p_t \oplus b$, with $a = 39\mu\text{m GeV}$ as extracted from the simulation of multiple scattering and with the asymptotic value $b = 13\mu\text{m}$ extracted from the data after alignment.

Electron identification in CDF relies on the finely segmented central EM calorimeter, $\Delta\phi \times \Delta\eta = 15^\circ \times 0.11$. In the region $|\eta| < 1.1$ proportional wire chambers (CES) with cathode strips perpendicular to the wires are embedded at shower maximum, six radiation lengths deep inside the calorimeter. The CES measure the lateral shape and position of the EM showers and are used for electron and photon identification. Good electrons are defined by requiring that:

- only one track points to the calorimeter cluster,
- the ratio of the calorimeter energy to the track momentum satisfies $0.75 < E/P < 1.4$;
- the ratio of the energy deposited in the hadronic and EM compartments be $HAD/EM < 0.04$;
- the energy sharing with adjacent towers must agree with the expected lateral shower profile;
- the shower position measured by the CES must match the extrapolated CTC track; the shower shape must be compatible with a single electron as measured in the test beam.

During the 1988-89 data taking, two electron triggers the E_t thresholds of 7 and 12 GeV were used, collecting (0.22 ± 0.02) and $(4.2 \pm 0.3) \text{ pb}^{-1}$, respectively.

There are several different channels which allow the detection of b quarks. Fully reconstructed exclusive decays of b -hadrons allow the unambiguous tagging of a b -quark, together with a precise measurement of the hadron momentum. Viable examples are provided by $B^\pm \rightarrow J/\psi K^\pm$, $B^0 \rightarrow J/\psi K^*$ and $B^0 \rightarrow J/\psi K_S$. CDF had already detected during the 1988-89 run a total of 35 ± 9 events in the first two channels [3], and has now more 150-200 in all three channels (see Section 5). The capability to reconstruct such exclusive decays, in particular the $B^0 \rightarrow J/\psi K_S$ channel, is needless to say a milestone for any attempt to measure CP violation.

Due to the small branching ratios (BR) these channels are only accessible near threshold where the production rate of b quarks is more abundant. The region of small p_t is expected to be more sensitive to the uncertainties in the calculations mentioned previously and is therefore potentially more interesting for critical tests of QCD. At larger values of

p_t (typically above $10\div 15$ GeV) semileptonic decays become the leading tool to study b production. Neglecting detector backgrounds, and neglecting W , Z and c decays, b quarks are the most abundant source of high p_t leptons. Fig. 1 shows the inclusive electron p_t spectrum from the 1988-89 data.

Backgrounds from Z 's, W 's and continuum Drell-Yan events can be identified because single leptons from these processes are more isolated than leptons from heavy quark decays, surrounded by the fragments of a jet. In addition, lepton pairs from Z 's can be eliminated with a cut on the invariant mass of the lepton pair, and W 's can be identified by the large missing E_t and transverse mass of the $\ell\nu$ pair. Conversion electrons from $\gamma \rightarrow e^+e^-$ and from $\pi^0 \rightarrow \gamma e^+e^-$ are removed with 50% efficiency looking for a partner track with small opening angle with the candidate electron. The unseen conversions, where the soft electron partner cannot be found, are evaluated to be $(17 \pm 3)\%$ using a sample of conversion pairs identified independently. The fake hadron background is estimated to be $(17 \pm 5)\%$ from the distribution of the hadronic energy fraction.

For p_t values larger than $10\div 15$ GeV, the c and b cross sections are comparable. Since b quarks undergo a harder fragmentation into hadrons compared to c quarks, and since B hadrons have a larger phase space available for the decay, we expect the c contamination to contribute only a fraction of the total lepton yield. This fraction can be estimated by several means. UA1 studied the transverse momentum of the lepton relative to the direction of the jet in which it is imbedded (p_t^{rel}) [4]. At CDF the excellent tracking capability allows good mass resolution for charged final states. One can therefore tag the charmed hadrons (say D 's) near the electron. Fig. 2 shows the $D^0 \rightarrow K\pi$ peak from the prompt electron sample from the decay $B \rightarrow e\nu DX$ [5]. Fig. 3 shows the $K - \pi$ mass spectra in the $K^*(890)$ region for *right sign* combination to come from b decay ($e^- \bar{K}^{*0}$) and for *wrong sign* ($e^- K^{*0}$) combinations. A clear peak in the right sign channel is seen. The observed K^* rate agrees with what expected and provides a 30% upper limit on the charm fraction. The shape of the p_t^{rel} spectrum gives a charm fraction of $(20 \pm 10)\%$. Several additional resonances can be detected in the electron sample, such as $\Lambda \rightarrow p\pi$ and $\phi \rightarrow K^+K^-$ (Fig. 4).

b quarks can also be tagged through the inclusive J/ψ and ψ' signal, as a significant fraction of J/ψ 's and almost all of the ψ' 's are expected to originate from b decays. The reconstruction of a secondary vertex from which these ψ 's originate, made possible by the SVX, uniquely tags these events as b production (see Section 5).

2 B Production Properties

Heavy quark production in high energy hadronic collisions is fundamental for the study of perturbative QCD [6]. The comparison of experimental data with the predictions of QCD provides a necessary check that the ingredients entering the evaluation of hadronic processes (partonic distribution functions and higher order corrections) are under control and can be used to evaluate the rates for more exotic phenomena or to extrapolate the calculations to even higher energies. The estimates of production rates for the elusive top quark rely on the understanding of heavy quark production properties within QCD.

At the same time, the observability in hadron collisions of CP violation in the B

system [1] as well as other phenomena such as B_s mixing or rare decays, depends to a large extent on the production cross section and correlations between the B and \bar{B} .

Complete NLO calculations are available today for the total [7], one-particle-inclusive [8] and two-particle-inclusive [9] cross sections. Production of heavy quarks in the perturbative evolution of high energy jets has also been studied, and LO expressions for the heavy quark multiplicities are known [10].

When applied to the energy of the current hadron colliders, these results are believed to provide a reliable description of the production properties of very massive quarks – e.g. the yet undetected top . In the case of *charm* and *bottom*, the situation is more delicate. In fact production of c and b quarks is dominated by gluon fusion processes ($gg \rightarrow Q\bar{Q}$) and the distribution of gluons inside the proton is probed at values of x close to the boundary of current DIS measurements. Furthermore the next-to-leading order (NLO) contribution is larger than the leading order (LO) result, and very sensitive to the input scale μ . Significant corrections are thus expected from yet higher order terms.

The b -quark integrated p_t distribution measured by CDF using the channels discussed above is presented in fig. 5, where the acceptance driven cut $|y| < 1$ is understood. The data are all taken from the analyses of the 1988-89 data [3, 5], [11]-[14], and work is in progress on the new data.

The data are compared with the results of the NLO QCD calculation [8], evaluated [15] using the most recent MRS parton distribution function (PDF) fits [16] of the NMC [17] and CCFR [18] data. The two theory curves correspond to different values of the renormalization scale μ_F and Λ_{QCD} , namely: $\Lambda_{QCD}=215$ MeV, $\mu_F=m_T$ and $\Lambda_{QCD}=275$ MeV, $\mu_F=m_T/4$. These choices, with $m_T^2 = p_t^2 + m_b^2$, represent a rather extreme although acceptable range for the values of the parameters, and the relative curves represent the presumed range within which the NLO QCD prediction is allowed to vary.

There is a clear excess in the observed rate at small p_t . At larger values of p_t , in the region of the inclusive $b \rightarrow l + X$ measurements, the data are consistent with the upper extreme of the theoretical band.

2.1 Implications of the Measurement

The b cross section measurement at 1.8 TeV is clearly an important benchmark to establish feasibility of CP violation measurements at high energy hadron colliders. The UNK energy, 2.2 TeV in the center of mass, is close enough to 1.8 TeV that the CDF measurement would serve as a very accurate engineering number for those interested in that project. However the proposed experiments [19] will work in a *forward* geometry, therefore probing a region of p_t almost complementary to the one probed by CDF. The 4π detectors at LHC [20] will probe values of x ten times smaller than those probed by CDF. How reliable are therefore extrapolations based on the CDF results? While we cannot answer this question, we will address some aspects of it in this Section.

We will start with some comments regarding the possibility to extrapolate a measurement performed in the p_t range of CDF to $p_t=0$. For the time being we neglect the observed disagreement between data and QCD, and just work within the framework of the NLO calculation and its intrinsic and understood uncertainties, namely possible m_b , μ_F and PDF variations.

As a reference we will use sets D0 and D- of the recent MRS PDF parametrization [16]. We will use two values of Λ_{QCD} , $\Lambda_0=215$ MeV and $\Lambda_+=275$ MeV, corresponding respectively to the central value and to one standard deviation above the central value obtained from the fit. Tables 1 and 2 contain the bottom quark p_t distribution integrated above a given p_t at 1.8 TeV and for the two extreme values of μ_F , $\mu_F=m_T$ and $\mu_F=m_T/4$. The quark is required to satisfy $|y| < 1$.

Several comments are in order. First of all notice that the use of the more singular set of structure functions leads to larger values of the total cross sections ($p_t > 0$) at 1.8 TeV. On the other hand, the singular gluon parametrization D- will give a cross section smaller than the set D0 as soon as we consider transverse momenta of the b above 10 GeV, which is the region where most of the CDF data are. This is because the higher density of gluons at small x described by set D- forces via momentum sum rules a depletion at larger values of x . Since above 10 GeV the shapes of the integrated p_t distributions for the two parametrization D0 and D- are similar, this indicates that the measurement of the cross section for b production in this region cannot be reliably used to extrapolate to $p_t=0$ the total b production cross section. For example, while the region $p_t > 10$ GeV represents 10% of the total cross section according to D0 and using $\Lambda_{QCD}=215$ MeV, the same region represents only 7% of the total according to D- and using $\Lambda_{QCD}=275$ MeV.

As already indicated in [8], the dependence on the value of the b mass is not significant. In Table 3 we show a comparison between the integrated b p_t distribution obtained using $m_b=4.5$ and $m_b=4.75$ GeV. The difference is of the order of 20% for the total cross section, but becomes negligible for $p_t > 10$ GeV.

We conclude that the extrapolation to the total b cross section from its measurement in the region $p_t > 10$ GeV has, even within NLO QCD, an uncertainty of the order of 50%. The extrapolation from the $|y| < 1$ region to the full rapidity interval is more solid, as it is mostly governed by phase space.

What about the observed disagreement between data and NLO QCD in the region $p_t \approx 10$ GeV? Is this factor of 3 discrepancy going to affect directly the total cross section? Does this indicate a more rapid growth of the total cross section than predicted by NLO QCD? The suggestion has often been made that our ignorance on the gluon PDF in the small- x region could be responsible for this disagreement. Rather than studying this possibility by directly attempting to modify the gluon densities to fit CDF data, as done in refs.[21, 22], we will consider here the following quantity:

$$\sigma(x_g < x; p_t^b > p_t^{min}) = \int_0^x dx_g \frac{d\sigma(p_t^b > p_t^{min})}{dx_g}, \quad (1)$$

namely the contribution to the integrated p_t distribution coming from partons with momentum fraction smaller than a given value of x . We plot this variable as a function of x and for different values of $p_t^{min}(b)$ in Fig. 6. We only integrated over b quarks within the regions of acceptance of the experiment, namely $|y_b| < 1$. Since the contribution to the cross-sections due to the $q\bar{q}$ and gq initial states are negligible for the relevant regions of p_t we are concerned with, we limited ourselves to the gg process and normalized the curves to the value of 1 at $x = 1$. Therefore the plotted functions represent the fraction of cross-section due to gluons with $x_g < x$.

Notice that the contribution to the cross section for $p_t > 10$ GeV from the region

$x < 0.01$ is less than 20%. Furthermore no contribution at all comes from the region $x < 0.003$. We verified elsewhere [23] that different fits of the NMC and CCFR data, obtained in Ref. [24], give gluon densities which differ, over the relevant kinematic range, by no more than 10% from the MRSD0 set used here. Since all of these gluon parametrizations do not differ significantly from previous extrapolations, we conclude that the knowledge of the gluon density in the relevant region $0.1 > x > 0.01$ and $Q > 5$ is today rather solid. We therefore expect that only dramatic changes in the gluon densities in the region $0.003 < x < 0.01$ will lead to a change of a factor of 2 in the cross section integrated above $p_t = 10$ GeV.

Therefore while it is tempting to conjecture that the ignorance about the behaviour of the gluon densities at small- x could explain the difference in slope of the CDF spectra compared to theory, we find no evidence that this assumption is justified. Rather, we find that the region $x_g < 0.01$ is marginal in the production of b quarks passing the required acceptance and p_t cuts.

As an alternative explanation, recent theoretical work [25] has suggested that higher order small- x corrections to the partonic cross-section could increase significantly the heavy quark cross section. These phenomena alter the kinematic connection between p_t and x , since they predict that initial state gluons with a given momentum fraction x can have a p_t non negligible w.r.t. $x E_{beam}$. This is equivalent to having an intrinsic p_t of the order of the scale of the hard process itself, namely m_b . As a result, the region with $x_g < 0.01$ could provide a significant contribution to the rate for $p_t^b > 10$ GeV, thanks to the transverse momentum smearing induced by this sort of *small- x primordial* p_t . Even though it was found in ref.[25] that these small- x effects can add at most 50% of the NLO contribution to the total b cross section at 1.8 TeV, no explicit indication is given on the p_t distribution of this additional 50%. Since the cross section observed experimentally ($p_{tb} > 8.5$ GeV) represents of the order of 10% of the total rate at NLO, we cannot exclude that the p_t smearing induced by these effects be responsible for the factor of 2-3 discrepancy observed between data and NLO predictions. Notice that the hypothesis of a p_t smearing would help understanding not just the rate deficiency, but also the apparent difference in shape between NLO and data.

If these mechanisms were at work, therefore, the observed difference between data and the NLO prediction would not affect the total cross section as much as it affects the partial $p_t > 10$ GeV rate, and it would be wrong to assume that total cross sections should be larger than NLO QCD by a factor of 3 in extrapolating to $p_t > 0$ or to higher energy.

A quantitative statement regarding these possibilities will only come from more explicit studies. While we await for new calculations, it might be worth exploring some additional consequences of this scenario. In addition to trying to push the measurement of the b cross section to even smaller values of p_t , it would be important to study correlations between the pair of b quarks. NLO calculations exist for these correlations [9]. If the small- x effects were to behave as indicated previously, we would expect to observe a flattening of the $\Delta\phi$ and $p_t^{b\bar{b}}$ distributions w.r.t the NLO prediction. Here $\Delta\phi$ represents the difference in azimuth between the b and the \bar{b} , and $p_t^{b\bar{b}}$ represents the transverse momentum of the pair. The flattening would be caused by the additional intrinsic p_t due to the gluon transverse momentum.

Measurements of the $\Delta\phi$ correlations have been performed by UA1 [26], indicating

a good agreement with the NLO calculation [9]. This result does not resolve the issue, though, because the agreement of the NLO b cross section with the data at UA1 suggests that the energy at UA1 is below the threshold for the possible onset of these new small- x phenomena.

Similar studies are in progress at CDF using the new data, and will hopefully lead to a better understanding of this important issue, as well as provide a more solid basis for the understanding of correlations between b and \bar{b} pairs, necessary in any study requiring double tagging.

3 Charmonium Production

The theory of quarkonium production [27] is on a less solid ground than the theory of open heavy-quark production. Production cross sections are evaluated by convoluting the $c\bar{c}$ matrix elements with the non-relativistic charmonium wave function, parametrized in terms of the decay widths of the relevant (J, L) state. The QCD radiative corrections to the LO processes have not been evaluated yet.

The observation of J/ψ 's is however an important ingredient in the study of b production. On one hand, a significant fraction of the detected J/ψ 's comes directly from b -hadron decays rather than from prompt charmonium formation [28, 4]. In fact the J/ψ form factor inhibits production with $p_t \gg m_c$. On the other hand, b -decay final states involving a J/ψ provide unique tags in the search of yet unobserved or rare b -hadrons (such as B_s, B_c, Λ_b) as well as in the detection of CP asymmetries (e.g. from $B_d \rightarrow J/\psi K_S^0$ decays [1].)

3.1 J/ψ and ψ' production

The measurement of the J/ψ and ψ' production cross section reported here is based on a recently completed analysis of $2.6 \pm 0.2 \text{ pb}^{-1}$ of data collected during the 88/89 run. The sample consists of events with two muons with $p_t > 3 \text{ GeV}$ each and contained within $|\eta| < 0.5$. The muon pair is required to have $p_t > 6 \text{ GeV}$. The invariant mass distribution in the regions around the J/ψ and ψ' is shown in fig. 7. The number of J/ψ candidates above background and within a $\pm 2.5\sigma$ mass signal region, $3.05 < m_{\mu^+\mu^-} < 3.15$, is 889 ± 30 . The resulting J/ψ mass is $(3.0965 \pm 0.0007) \text{ GeV}$, with a width of $(18.5 \pm 0.6) \text{ MeV}$. The number of ψ' candidates above background and within a $\pm 2.5\sigma$ mass signal region, $3.63 < m_{\mu^+\mu^-} < 3.73$, is 35 ± 8 . The resulting ψ' mass is $(3.683 \pm 0.005) \text{ GeV}$, with a width of $(20 \pm 4) \text{ MeV}$.

The largest systematic uncertainty in the measurement of the cross section, after accounting for trigger and track finding/reconstruction efficiencies [11], comes from the uncertainty in the trigger efficiency ($\pm 9\%$ on the cross section). An additional systematic uncertainty is related to the polarization state of the J/ψ . While direct J/ψ 's are expected to be unpolarized, this is not the case for J/ψ 's coming from the decay of a B meson. Polarized J/ψ 's would produce muons with a different p_t spectrum, therefore affecting the estimate of the trigger acceptance. Assuming conservatively that all J/ψ 's come from B 's, and exploring the range of extreme choices for the decay polarization of the J/ψ 's,

we estimate a systematic uncertainty on the J/ψ (ψ') production cross section of ${}_{-11.2\%}^{+6.5\%}$ (${}_{-7.3\%}^{+4.4\%}$).

The measurements result in the following cross sections:

$$BR(\psi \rightarrow \mu^+ \mu^-) \times \sigma_\psi(p_{t\psi} > 6\text{GeV}; |\eta| < 0.5) = 6.88 \pm 0.23(\text{stat}) {}_{-1.08}^{+0.93}(\text{syst}) \text{ nb} \quad (2)$$

$$BR(\psi' \rightarrow \mu^+ \mu^-) \times \sigma_{\psi'}(p_{t\psi'} > 6\text{GeV}; |\eta| < 0.5) = 0.232 \pm 0.051(\text{stat}) {}_{-0.032}^{+0.029}(\text{syst}) \text{ nb} \quad (3)$$

These numbers can be turned into a measurement of the b cross section by assuming that a given fraction f_B of the J/ψ 's come from B decays, and correcting for the acceptance using a MC model based on the NDE p_t^b spectrum [8] and ARGUS+CLEO ($B \rightarrow \psi, \psi'$) spectra. Taking $f_B=1$ we calculate:

$$\sigma(p\bar{p} \rightarrow b X \quad p_t^b > 8.5\text{GeV}; |y| < 1) = 18.9 {}_{-5.0}^{+4.7} \mu\text{b} \quad \text{using } \psi\text{'s} \quad (4)$$

$$\sigma(p\bar{p} \rightarrow b X \quad p_t^b > 8.5\text{GeV}; |y| < 1) = 10.5 {}_{-5.1}^{+5.0} \mu\text{b} \quad \text{using } \psi\text{'s} \quad (5)$$

The two measurements shown in fig. 5 are plotted assuming $f_B = 1$ for the ψ' and $(63 \pm 17)\%$ for the J/ψ . The first value is justified by theoretical expectations, the second was derived assuming that all non- B J/ψ 's come from χ decay (see next Section).

Figure 8 shows the inclusive p_t differential distribution for J/ψ 's measured by CDF [11]. We superimpose the result of a QCD calculation [15] based on the LO matrix elements given in Ref. [27] for the direct charmonium production, plus the contribution from B decays evaluated using NLO matrix elements [8], convoluted with a Peterson fragmentation function and the $B \rightarrow J/\psi$ decay spectrum observed by CLEO and ARGUS. The theoretical error band is evaluated using the same range of parameters Λ_{QCD} and μ employed before in the study of the b cross sections. Notice that changing μ for the direct charmonium contribution causes a variation ranging from a factor of 7 to 10, depending on p_t . This indicates that the LO prediction for direct charmonium is very poor, and very large NLO corrections should be expected.

CDF data show a production rate larger than expected. Equally worrisome is the comparison between theory and data in the case of the p_t spectrum of the ψ' , shown in fig. 9. As noted in [11, 28], the expected contribution from direct quarkonium production is heavily suppressed, and the figure indicates that this remains true even allowing for the variation of μ_F within the $\mu_0/4 < \mu_F < \mu_0$ range.

In Table 4 we present the integrated p_t distribution of J/ψ mesons, calculated at CDF energy and divided into the direct quarkonium and B decay contributions. The relative fraction due to B decays, f_B , is also shown as a function of the p_t threshold, and the dependence on Λ_{QCD} and μ_F is studied by considering the central case of $\Lambda_{QCD}=215$ MeV, $\mu_F=m_T$ and the extreme case of $\Lambda_{QCD}=275$ MeV, $\mu_F=m_T/4$. A priori there is no reason why the same factorization scale should be used for the two contributions, as the two physics processes are entirely different. Furthermore the B decay is evaluated at NLO, while as mentioned previously only the LO terms are available and included in the quarkonium term. Nevertheless we take here the value of μ for the two processes to be the same, in order to extract an indicative range of values for f_B .

The value of f_B plays an important role in the experimental determination of the B cross section out of the measurement of the inclusive J/ψ rate. The right hand side of Table 4 – which represents the choice of parameters which comes closer to representing the CDF J/ψ spectrum – suggests a value for f_B which is significantly smaller than used in fig. 5. This would decrease the effective b cross section by a factor of 50%. The range of values exhibited by the tables indicates what is the systematic uncertainty that one should expect in deriving f_B from the theory.

f_B can be extracted experimentally by other means, for example by separating the direct J/ψ 's from those due to B decays via the observation of the displaced vertex from which the J/ψ originates, due to the long B lifetime. We will present a preliminary measurement of f_B carried out using this technique in the Section on the B lifetime.

Alternatively UA1 measured f_B (32% for $p_t(\psi) > 5$ GeV [4]) by assuming that direct J/ψ 's are isolated while J/ψ 's from B decays are not. This number is consistent with the estimates provided in [15]. The assumption used by UA1 to extract f_B however might not be correct if other production mechanisms were responsible for direct quarkonium production, such as for example gluon $\rightarrow J/\psi$ fragmentation [29]. It is reasonable to expect that at some value of p_t the dominant production mechanism for charmonium states will indeed be via gluon fragmentation. The main reason being that direct production as described by the LO mechanisms inhibits production at large p_t via a form factor suppression (the probability that a charmonium bound state will hold together when produced *directly* in an interaction with a large virtuality scale is highly suppressed). The fragmentation functions for the creation of S -wave charmonium (η_c and J/ψ) in a gluon shower have recently been calculated [29] and those for the creation of P -wave states (χ) will soon be available (E Braaten & TC Yuan, personal communication).

These calculations can be used to extract the fragmentation contribution to charmonium production in the regions of p_t explored experimentally, and to verify whether this process can account for the large observed rates. The experimental detection of non-isolated J/ψ 's from a primary vertex, therefore not coming from B decays, would indicate that these processes are indeed present. Along the same lines, measurements of the decay-vertex position of the ψ' would provide evidence in favour or against the current belief that most of them come from B decays. If the gluon fragmentation mechanism were important, it would appear with a signal of non-isolated prompt ψ' .

Both these studies are in progress at CDF using the new data. The current sample of J/ψ 's is significantly larger than what available for the analyses presented above, and statistical as well as systematic errors will decrease substantially in the forthcoming studies.

3.2 χ detection and cross section measurement

An additional important ingredient in this picture is the production of χ states. This is expected to be dominated by direct production rather than B decays. CDF has fully reconstructed χ_c mesons through the decay chain $\chi_c \rightarrow J/\psi\gamma$, $J/\psi \rightarrow \mu^+\mu^-$, for the first time in hadronic collisions. We will shortly summarize here the results of the recently completed analysis from the 88-89 data [14].

The starting sample is the same as employed in the J/ψ study discussed above. Photon

candidates are selected by requiring an EM energy cluster in excess of 1 GeV and a cluster in CES. The direction of the photon is defined by the position of the cluster on the strip chambers and by the muon pair vertex. The mass difference of the $\mu\mu\gamma$ system and the $\mu\mu$ pair is then plotted (figure 10) and shows a clear peak at a mass of 406 ± 13 MeV. This value is consistent with the masses of the χ_1 and χ_2 states, which are indeed expected to dominate the observed mode because of the small branching fraction of the $J = 0$ state (χ_0) into muons. The observed signal corresponds to 67 ± 8 (statistical) events within one standard deviation of the expected average mass. From this signal we can extract a cross section measurement after evaluating the detection efficiencies. This results in

$$BR(\psi \rightarrow \mu^+\mu^-) \times \sigma(\chi_c \rightarrow \psi\gamma; p_{t\chi} > 7\text{GeV}; |\eta| < 0.5) = 3.2 \pm 0.4 \pm 1.1\text{nb} \quad (6)$$

This measurement can be compared with the range $0.64\text{nb} < \sigma < 5.1\text{nb}$ obtained using the LO QCD calculation described above for the J/ψ 's [15].

We can use our measurement of the χ production cross section to evaluate the expected rate of observed J/ψ 's from χ decays. Assuming that no significant direct J/ψ production is present, as is expected from the LO calculations, we can obtain by difference the number of J/ψ 's coming from B decays, and therefore an estimate of the b cross section. This results in [14]:

$$\sigma^b(p_t^b > 8.5\text{GeV}, |y^b| < 1) = 12.0 \pm 4.5\mu\text{b}, \quad (7)$$

which is consistent with the values quoted previously. The resulting value for f_B is $f_B = 63 \pm 17\%$.

The additional statistics available from the 92-93 data will allow a more precise study of this important channel. In particular, enough statistics will be available to derive a p_t distribution of χ 's, and the SVX will allow a study of the position of the decay vertices. If all χ 's were prompt, no tail in this distribution should be observed. Given the observed branching ratio for $B \rightarrow \chi X$, $0.54 \pm 0.21\%$ [30], we expect a small fraction of χ 's coming from B decay (less than 10%). This should leave a tail in the position of the decay vertex. It will also be interesting to study the distribution of tracks surrounding the prompt χ 's, to determine whether they are produced directly or via a gluon fragmentation mechanism.

4 Inclusive B Lifetime

The CDF experiment has already collected several thousand J/ψ 's since the start of the ongoing collider run. The size of the sample and the very good spatial resolution of the SVX allow a precise measurement of the inclusive B lifetime. In the following we will describe the basic guidelines of this analysis and its preliminary results.

The basic idea for this analysis is that it is possible to separate in a simple way the contribution of J/ψ 's from B decays from those originating from other sources. Indeed there are just 3 sources:

- a) J/ψ from B decay,
- b) J/ψ from direct production or via direct production of 0 lifetime intermediate states like χ 's and Υ 's,

- c) false J/Ψ simulated by 2 μ 's originated by Drell-Yan pairs, or by the decay of different particles, or by misidentified muons, whose invariant mass falls by accident in the mass range around the J/ψ mass.

J/ψ 's of type a) have a decay length which is strictly related to that of the parent B hadron, so they are to some extent separated from the primary interaction vertex. Those of type b) come instead directly from the interaction vertex, and those of type c) represent a background, whose decay path characteristics are not so well defined, which can however be subtracted by studying the size and the shape of the J/ψ sidebands.

The measurement procedure consists therefore in an analysis of the shape of the J/ψ pathlength distribution, which takes into account the contributions of all these sources.

4.1 Definition of the J/ψ sample

The J/ψ 's used in this analyses are required to have both muons fully reconstructed within the SVX and at least one muon with $p_t > 2.5$ GeV. The second muon has an intrinsic p_t threshold of ≈ 1.4 GeV given by the amount of traversed hadron absorber. Because of the limited geometric acceptance of the SVX relative to the spread of the luminous region, the first requirement reduces the J/ψ sample by a factor of approximately 2.

A series of quality cuts is then applied to the SVX reconstructed muon tracks and to the fit for a common vertex. It is also required that the calculated error on the transverse decay length, error which varies event-by-event because of the different J/ψ decay configurations, be less than $150 \mu\text{m}$.

J/ψ 's are then defined by a mass window of ± 50 MeV around the J/ψ mass. The background in this mass range is 5–7% of the signal, depending on the track quality cuts and estimated by interpolating the side bands. These cuts leave us of the order of 5000 J/ψ 's out of the 13000 fully contained in the SVX currently analyzed (9pb^{-1}).

4.2 Definition of the pseudo- $c\tau$ variable

For most B's in the sample we cannot close the kinematics. It is therefore impossible to determine exactly both the $\beta\gamma$ correction and the precise direction of the B. It is however important for our study to define a variable which is as close as possible to the proper B lifepath. In the following we shall describe how this variable is constructed.

After fitting for the common vertex position of the two muons, \vec{x}_ψ , we define a signed transverse decay length, L_{xy} :

$$L_{xy} = \frac{\vec{R} \cdot \vec{p}_t^\psi}{|\vec{p}_t^\psi|},$$

with:

$$\vec{R} = \vec{x}_\psi - \vec{x}_{prim},$$

being the transverse decay length vector. Since the width of the beam line is seen to be of the order of $35 \mu\text{m}$, comparable with that expected for the event by event fit, but much more insensitive to systematics and more efficient, we have used this determination of the primary interaction vertex \vec{x}_{prim} throughout the analysis. Notice that here the

flight direction of the J/ψ and of the parent B are taken to be the same. A Monte Carlo study has shown that the opening angle between the B and the J/ψ is about 7° with a maximum value of 20° , implying an error of at most 5% due to this approximation.

We have now to correct L_{xy} for an approximate $\beta_t\gamma$ factor, in order to obtain a proper transverse decay length λ . Again we use the fact that the J/ψ is massive and we use the $\beta_t\gamma$ of the J/ψ as an estimate, applying a correction factor determined by MC:

$$\lambda_{corr} = L_{xy} \cdot \frac{M_\psi}{p_t^\psi F_{corr}(P_t^\psi)}$$

An exponential fit to the distribution of λ_{corr} and to the true λ shows a consistency of the slope at the 3% level.

4.3 The results

The distribution of the pseudo- $c\tau$ distribution is presented in fig. 11, showing a clear signal of positive lifetime. The shaded area corresponds to the background, whose shape and normalizations are determined by the study of the sidebands. Even this distribution shows a positive lifetime, as expected if part of the background is generated by sequential B decays. It was checked by MC that this is indeed the case.

The distribution is fitted using the sum of a gaussian term (direct J/ψ 's), a background term (sum of a gaussian, a left- and a right-side exponential) and an exponential convoluted with a gaussian (J/ψ 's from B decays). The parameters of the background distribution are fixed by the study of the side bands. The remaining parameters to be fitted are f_B and $c\tau$. As an alternative, one can decide to consider only the exponential tail for $\lambda_{corr} > 400\mu\text{m}$, having $c\tau$ as the only parameter.

The value obtained for f_B is of the order of 20%. The preliminary inclusive B lifetime is measured to be:

$$c\tau = 420 \mu\text{m} \pm 19\mu\text{m} (stat.) \pm 29\mu\text{m} (syst.).$$

This measured lifetime value is consistent with what measured by the LEP experiments [31].

4.4 Prospects for further lifetime and f_B studies in the current run

The systematic uncertainty on $c\tau$ is at this time dominated the parameterization chosen to describe the tails of the λ_{corr} distribution for the background. Additional statistics will allow to reduce this effect. The residual misalignment of the SVX, now responsible for a 2% systematic uncertainty, will eventually have a negligible effect after including the alignment corrections. Uncertainties in the modeling of the B production spectrum and J/ψ p_t distribution (now at the level of 3%), will also be reduced by directly using the data. Uncertainties in the $B \rightarrow \psi$ decay (momentum spectrum and polarization) are at the level of 1% if use is made of CLEO and ARGUS data. It is expected that the final total systematic uncertainty on $c\tau$ will be smaller than 5%.

The measured value of f_B is significantly smaller than what used in extracting the B cross section from the 88/89 J/ψ data. However the J/ψ 's in the data sample used for this analysis have a spectrum which extends to much smaller values of p_t than the 88/89 sample. A more detailed study of the p_t dependence of f_B is in progress, and will be used to shed more light on the b cross section issues mentioned in a previous section.

Similar studies are likewise in progress using the ψ' , benefiting from both the $\mu^+\mu^-$ and the $\psi\pi^+\pi^-$ decay channels. Given the current number of reconstructed ψ' in this last channel (192 ± 21 events in 9pb^{-1}), we estimate of the order of 550 events by the end of this run. Scaling up the number of ψ' detected in 88/89 in the muon channel, we expect at least another 1000 reconstructed in the SVX from this mode. This is consistent with a preliminary study of 2pb^{-1} of 1992 data, resulting in $\approx 100 \psi'$.

Using the relative number of χ 's reconstructed in the 88/89 data (≈ 60 out of a sample of 900 J/ψ 's, see Section 3), we expect by the end of the current run of the order of 1500–2000 χ 's fully reconstructed inside the SVX. This should suffice to determine a fraction of χ 's from B decays at the level of few per cent. The expected value of f_B^X is of the order of 5–10%.

Furthermore, the number of exclusive B decays reconstructed in the $B^\pm \rightarrow J/\psi K^\pm$, $B^0 \rightarrow J/\psi K^*$ and $B^0 \rightarrow J/\psi K_S$ modes will allow a determination of the separate charged and neutral B lifetime with a statistical accuracy of about 5%. Theoretical analyses of the inclusive $B \rightarrow e + X$ branching ratio [32] indicate that the difference between charged and neutral lifetimes should be of the order of 20%, which is therefore well within the reach of CDF.

5 B Exclusive Decays

CDF has shown already from the analysis of the 88/89 data a good capability to fully reconstruct exclusive decay modes of B mesons. The 35 ± 9 events detected in the $B^\pm \rightarrow J/\psi K^\pm$ and $B^0 \rightarrow J/\psi K^*$ modes, shown in fig. 12, were used to determine the B cross section [3, 12]. The addition of the SVX has significantly improved CDF's ability to reconstruct clean samples of these decays. In this section we present some very preliminary results of these studies from the 1992/93 data. The aim is solely to show how clean the signal can be, as no systematic attempt to optimize the efficiency of the cuts has been made.

The J/ψ sample consists of ≈ 27000 J/ψ 's, corresponding to 9pb^{-1} of data. About half of these are fully reconstructed in the SVX. The mass distribution for a slightly smaller subsample is shown in fig. 13. We then use dimuons within 80 MeV of the J/ψ mass. To these J/ψ 's, we combine tracks which pass minimal track quality cuts. We perform a combined vertex constraint with a J/ψ mass constraint and a pointing constraint to the primary vertex.

In addition, we require the following:

- p_t of the K^\pm (K^*) greater than 2 GeV;
- p_t of the B_u (B_d) greater than 8 GeV;
- Lifetime, $c\tau$, greater than 100 μm ;

- Fit χ^2 less than 100;
- $K\pi$ mass within 80 MeV of the K^* mass.

In case of ambiguity for the K^* , we use the $K\pi$ closest to the K^* mass. The resulting mass spectra are shown in fig. 14 and 15. To display the power of the lifetime cut, we show the mass distribution of the ψK^\pm mode with and without the $c\tau$ cut in fig 16 (the upper plot refers to SVX and CTC, the lower plot SVX only). Here the p_t cut for the B was reduced to 6 GeV.

In Table 5 we collect the preliminary values of some of our mass fits, and compare them to the world averages. The results for the ψ' refer to the $\psi' \rightarrow \psi\pi\pi$ decay mode. This is reconstructed with a technique similar to what described above, but for the pointing to the primary vertex, which is not demanded in this case as ψ' 's are expected to come mostly from B decays. The ψ' mass plots are shown in fig. 17. Approximately 20 $B \rightarrow \psi K_s$ have also been reconstructed already, but are not shown here.

Studies are in progress to reconstruct a sample of exclusive $B_s \rightarrow \psi\phi$ decays, where we expect to observe a signal of few tens of events by the end of the run, sufficient for a first estimate of the B_s mass. Limits have been set from the 1988/89 data on the production of Λ_b [33]. CDF limits seem to be stronger than the production rate reported by [34], and the search for this state is continuing using the new data sample. As for the observation of other new states, as an example we include here a short summary of the discovery potential for the B_c state, and refer to the report of the Theory Group at this Workshop for more details [35].

5.1 Prospects for B_c Discovery at CDF

Bound states of a b and \bar{c} quark pair have never been observed. They represent interesting objects for QCD because their properties are expected to be calculable on the basis of what already known of $c\bar{c}$ and $b\bar{b}$ states. Possible differences between different models, such as non-relativistic potentials or QCD sum rules, can therefore be tested. Estimates of the mass of the lowest energy state (the B_c (0^-) meson) vary in the range $M_{B_c} = 6250 \pm 100$ MeV [36], depending on the details of the model. The splitting between the ground state and the vector B_c^* is rather model independent, and of the order of 80 MeV [36]. We will however concentrate here on the 0^- state only.

From the point of view of the detection, the two most important parameters are the production rate and the branching ratios (BR) into accessible decay modes. The production rate can be expressed in terms of the fraction of b quarks that will evolve into a B_c meson, $f_{(b \rightarrow B_c)}$. No complete calculation of this parameter is available as yet, but partial estimates have been carried out [37]. A reasonable range is $f_{(b \rightarrow B_c)} = 1 \div 5 \times 10^{-3}$, combining both perturbative and non-perturbative contributions.

The situation with BR's is likewise uncertain. The results of potential models and QCD sum rules seem to differ on the value of the pseudoscalar decay constant (f_{B_c}), and on the values of the most interesting BR's [38]. We collect some of these results in Table 6. Notice that also the lifetime has a rather large range of values. This is a critical parameter in view of the possibility to reduce the background to the decay modes via the presence of a secondary vertex.

In order to get a crude estimate of the possible signal at CDF, we will normalize ourselves to the number of observed exclusive B decays. The best decay channel that allows full reconstruction is $B_c \rightarrow \psi\pi^+$. We will confront this channel to the observed $B_u \rightarrow \psi K^+$, assuming equal acceptance and reconstruction efficiency. Notice however that the efficiency for the B_c decay is expected to be higher; in fact, the larger mass of the B_c w.r.t the B^+ and the smaller mass of the pion w.r.t kaon will give a larger impact parameter and a higher transverse momentum to the decay pion.

Under the assumption of equal efficiency, we can write the following equation for the number of expected reconstructed decays (the subsequent $\psi \rightarrow \mu^+\mu^-$ decay is understood):

$$\frac{(B_c \rightarrow \psi\pi^\pm)}{(B^+ \rightarrow \psi K^\pm)} = \frac{f_{(b \rightarrow B_c)}}{f_{(b \rightarrow B_u)}} \times \frac{BR(B_c \rightarrow \psi\pi^\pm)}{BR(B^+ \rightarrow \psi K^\pm)} \approx 6 f_{(b \rightarrow B_c)}, \quad (8)$$

where we used the value of the BR given in Table 6 and $f_{(b \rightarrow B_u)}=35\%$. Using the number of currently reconstructed $B \rightarrow \psi K^\pm$ (approx. 60 events in 9pb^{-1}), we obtain $N(B_c \rightarrow \psi\pi^\pm) \approx 360 f_{(b \rightarrow B_c)}$. This corresponds to 1–5 events in 25pb^{-1} , using the range of estimates for $f_{(b \rightarrow B_c)}$. Considering the levels of the combinatorial background, this signal could be detected with a larger integrated luminosity only in the upper range of $f_{(b \rightarrow B_c)}$, unless the detection efficiency is significantly higher for this mode than for $B \rightarrow \psi K$.

One could also hope to establish the presence of a B_c signal by looking at the inclusive $B_c \rightarrow \psi\ell\nu$ decays, observing the presence of the third lepton coming from the same secondary vertex as the ψ . In this case we can write:

$$\frac{(B_c \rightarrow \psi e(\mu)X)}{(B \rightarrow \psi X)} = \frac{f_{(b \rightarrow B_c)}}{f_{(b \rightarrow B)}} \times \frac{2BR(B_c \rightarrow \psi\ell X)}{BR(B \rightarrow \psi X)} \approx 20 f_{(b \rightarrow B_c)}. \quad (9)$$

This indicates that of the order of 2–10 % of the ψ 's from B decays could be accompanied by an additional lepton (e or μ). The requirement that this lepton come from the same vertex as the ψ and with a large p_t relative to the direction of the B should reduce significantly the possible background, but accurate feasibility studies are still lacking. In equation (9) we used the PM estimate of the inclusive $B_c \rightarrow \ell\nu$ decay. The SR estimate would give a smaller, and perhaps unobservable, signal.

6 Conclusions

Some of the earlier CDF results we could not review here for lack of time. This is the case of $B\bar{B}$ mixing [41] and $B \rightarrow \mu^+\mu^-$ decays. A more precise measurement of $B\bar{B}$ mixing with the new data, together with the accurate measurement of B_d mixing from CLEO and ARGUS, will allow a determination of the B_s production rates, to be compared as an important consistency check with the observed cross sections. The background rejection power of the SVX will allow to extend even further the limits on the $B \rightarrow \mu^+\mu^-$ branching ratios. Systematic studies to establish the ultimate achievable limit are in progress.

The B physics program of CDF is in continuous evolution, as the new elements of the detector are better understood and new upgrades are being undertaken. It is hard to estimate today what the final B physics reach of CDF will be, as economic pressures on both the experiment and the Laboratory make it difficult to rely on the most optimistic

upgrade scenarios. Nevertheless we believe that the results obtained so far provide a strong proof that complex B physics can indeed be performed in hadronic collisions with good efficiency and sufficient background rejection.

The current and forthcoming runs of CDF will provide essential information on the production mechanisms for b quarks and J/ψ mesons. These studies will hopefully solve the long standing debate on the reliability of NLO QCD to evaluate the b cross section, and will stimulate continuous efforts by the theorists to improve the calculations. As a result, we hope that reliable extrapolations of the b cross sections to the higher energies considered during this Workshop will become possible.

Large statistics of fully reconstructed B decays will allow direct experimental measurements of most of the key ingredients needed to evaluate the capability of an experiment in hadron collisions to perform delicate measurements such as CP violation or B_s mixing. For example, tagging efficiencies for the leptons in $B\bar{B}$ events with one B fully reconstructed will be measured in the large $B \rightarrow \psi K^\pm$ and $B \rightarrow \psi K^*$ samples. These efficiencies will strongly depend on the correlation properties of the B pairs produced, and therefore will also provide additional tests of QCD.

Acknowledgements: It is a pleasure to thank all my friends and colleagues at CDF for giving me the opportunity to present these results. I should thank in particular all those who directly contributed to my understanding of the results and who provided me with the relevant material: F. Bedeschi, F. De Jongh, V. Papadimitriou, P. Tipton, A. Yagil, W. Wester, A.B. Wicklund. Finally, I wish to acknowledge the organizers of this Workshop for the efforts made to guarantee its success and for the hospitality.

References

- [1] Nir Y, Quinn HR, *Annu. Rev. Nucl. Part. Sci.* **42** (1992), 211
- [2] F. Abe, et al., (CDF), *Nucl. Instr. Meth.* **A271** (1988), 387.
- [3] F. Abe et al., CDF Coll., *Phys. Rev. Lett.* **68** (1992), 3403.
- [4] C. Albajar et al., UA1 Coll., *Phys. Lett.* **256B** (1991), 121, *Phys. Lett.* **256B** (1991), 112.
- [5] F. Abe, et al., (CDF), CDF/PUB/HEAVYFLAVOUR/1653, submitted to *Phys. Rev. Lett.* (1993)
- [6] P. Nason, 'Heavy Quark Production', to appear in "Heavy Flavours", Advanced Series on Directions in High Energy Physics, ed. M Lindner, AJ Buras. Singapore: World Scientific (in press).
- [7] P. Nason, S. Dawson and R. K. Ellis, *Nucl. Phys.* **B303** (1988), 607;
W. Beenakker, H. Kuijf, W.L. van Neerven and J. Smith, *Phys. Rev.* **D40** (1989), 54.
- [8] P. Nason, S. Dawson and R. K. Ellis, *Nucl. Phys.* **B327** (1988), 49 ;
W. Beenakker, W.L. van Neerven, R. Meng, G.A. Schuler and J. Smith, *Nucl. Phys.* **B351** (1991), 507.
- [9] M. Mangano, P. Nason and G. Ridolfi, *Nucl. Phys.* **B373** (1992), 295.

- [10] Furmanski W, Petronzio R, Pokorski S, *Nucl. Phys.* **B155** (1979), 253;
Mueller AH, Nason P, *Nucl. Phys.* **B266** (1986), 265;
Mangano M, Nason P, *Phys. Lett.* **285B** (1992), 160.
- [11] F. Abe et al., CDF Coll., *Phys. Rev. Lett.* **69** (1992), 3704.
- [12] S. Vejjik, CDF Coll., presented at the 1992 DPF Meeting of the American Phys. Soc., Fermilab, November 11-14 1992.
- [13] B.T. Huffman, CDF Coll., presented at the 1992 DPF Meeting of the American Phys. Soc., Fermilab, November 11-14 1992; FNAL-CONF-92/337-E.
- [14] C. Boswell, CDF Coll., presented at the 1992 DPF Meeting of the American Phys. Soc., Fermilab, November 11-14 1992; FNAL-CONF-92/347-E.
- [15] M.L. Mangano, IFUP-TH 93/2 (1993).
- [16] A. Martin, R. Roberts and J. Stirling, RAL-92-021, DTP/92/16 (1992).
- [17] P. Amaudruz, et al., (NMC), CERN Preprint CERN-PPE/92-124.
- [18] S.R. Mishra, et al., (CCFR) Nevis Rep. NEVIS-1466 (1992); *Z. Phys.* **C53** (1992), 51
- [19] COBEX presentations, these Proceedings.
- [20] D. Denegri, Introductory and Concluding Remarks, to appear in these Proceedings; LHC presentations, these Proceedings.
- [21] E.L. Berger, R. Meng and W.K. Tung, *Phys. Rev.* **D46** (1992), 1895.
- [22] E.L. Berger, R. Meng and J. Qiu, ANL-HEP-CP-92-79.
- [23] J.E. Huth and M.L. Mangano, IFUP-TH 4/93, FNAL-PUB-93/19-E, to appear in *Annu. Rev. Nucl. Part. Sci.*, vol 43 (1993).
- [24] J. Botts, et al., (CTEQ), MSUHEP-92-27, Fermilab-Pub-92/371 (1992)
- [25] J.C. Collins and R.K. Ellis, *Nucl. Phys.* **B360** (1991), 3;
S. Catani, M. Ciafaloni and F. Hautmann, *Nucl. Phys.* **B366** (1991), 135;
E.M. Levin, M.G. Ryskin and Yu.M. Shabelsky, *Phys. Lett.* **260B** (1991), 429.
- [26] A. Geiser, presented at XXVII Rencontres de Moriond, Les Arcs, PITHA 92/19 (1992); PhD thesis. RWTH, Aachen (1992).
- [27] E.L. Berger and D. Jones, *Phys. Rev.* **D23** (1981), 1521;
R. Baier and R. Rückl, *Z. Phys.* **C19** (1983), 251;
B. Humpert, *Phys. Lett.* **184B** (1987), 105;
R. Gastmans, W. Troost and T.T. Wu, *Nucl. Phys.* **B291** (1987), 731.
- [28] E.W.N. Glover, A.D. Martin and W.J. Stirling, *Z. Phys.* **C38** (1988), 473;
E.W.N. Glover, F. Halzen and A.D. Martin, *Phys. Lett.* **185B** (1987), 441.
- [29] E. Braaten and T.C. Yuan, NUHEP-TH-92-23; UCD-92-25 (1992). K. Hagiwara, A.D. Martin and W.J. Stirling, *Phys. Lett.* **267B** (1991), 527.
- [30] R.A. Poling, in *Joint International Symposium and Europhysics Conference on High Energy Physics*, ed. S. Hegarty et al. (World Scientific, 1992), p.546.
- [31] E. Locci, in these Proceedings.
- [32] G. Altarelli and S. Petrarca, *Phys. Lett.* **261B** (1991), 308.
- [33] F. Abe et al., CDF Coll., FERMILAB-PUB-92-250-E, Sep 1992. Submitted to *Phys. Rev. Lett.*
- [34] Albajar C, et al., UA1 Coll., *Phys. Lett.* **273B** (1991), 540
- [35] A.K. Likhoded, S.R. Slabospitsky, M. Mangano and G. Nardulli, BARI-TH/93-137, Report of the Theory Working Group, in these Proceedings.

- [36] E. Eichten and F. Feinberg, *Phys. Rev.* **D23** (1981), 2724.
S. Godfrey and N. Isgur, *Phys. Rev.* **D32** (1985), 189.
S. S. Gershtein et al., *Sov. Jour. Nucl. Phys.* **48** (1988), 515.
P. Colangelo, G. Nardulli and M. Pietroni, *Phys. Rev.* **D43** (1991), 3002.
W. Kwong and J.L. Rosner, *Phys. Rev.* **D44** (1991), 212.
P. Colangelo, G. Nardulli and N. Paver, *Z. Phys.* **C57** (1993), 43.
E. Eichten and C. Quigg, to appear.
- [37] V. V. Kiselev, A. K. Likhoded and A. V. Tkabladze, *Sov. Jour. Nucl. Phys.* **46** (1987), 934.
M. Lusignoli, M. Masetti and S. Petrarca, *Phys. Lett.* **266B** (1991), 142.
- [38] V. V. Kiselev and A. V. Tkabladze, *Sov. Jour. Nucl. Phys.* **48** (1988), 536.
M. Lusignoli, M. Masetti and S. Petrarca, *Z. Phys.* **C51** (1991), 549.
V. V. Kiselev, A. K. Likhoded and A. V. Tkabladze A.V., Preprint IHEP 92-138 (1992).
- [39] N. Isgur, D. Scora, B. Grinstein and M. B. Wise, *Phys. Rev.* **D39** (1989), 799.
- [40] M. Wirbel, B. Stech and M. Bauer, *Z. Phys.* **C29** (1985), 637.
- [41] F. Abe et al., (CDF), *Phys. Rev. Lett.* **67** (3351), 1991.

Table 1: Integrated bottom quark p_t distribution at 1.8 TeV. $m_b=4.75$ GeV, $\mu_F=\mu_0$, $\Lambda_0 = 215$ MeV, $\Lambda_+ = 275$ MeV.

p_t^{min} (GeV)	MRSD0		MRSD-	
	Λ_0	Λ_+	Λ_0	Λ_+
0	1.14E+04	1.34E+04	1.33E+04	1.57E+04
5	4.50E+03	5.22E+03	4.50E+03	5.27E+03
10	1.05E+03	1.22E+03	9.45E+02	1.09E+03
15	3.16E+02	3.56E+02	2.70E+02	3.11E+02
20	1.15E+02	1.32E+02	9.69E+01	1.12E+02
25	4.97E+01	5.58E+01	4.20E+01	4.75E+01
30	2.40E+01	2.72E+01	2.06E+01	2.34E+01
40	6.94E+00	7.85E+00	6.05E+00	6.80E+00
50	2.60E+00	2.79E+00	2.16E+00	2.38E+00
59	1.21E+00	1.30E+00	1.03E+00	1.14E+00

Table 2: Integrated bottom quark p_t distribution at 1.8 TeV. $m_b=4.75$ GeV, $\mu_F=\mu_0/4$, $\Lambda_0 = 215$ MeV, $\Lambda_+ = 275$ MeV.

p_t^{min} (GeV)	MRSD0		MRSD-	
	Λ_0	Λ_+	Λ_0	Λ_+
0	2.17E+04	3.03E+04	2.69E+04	3.71E+04
5	7.23E+03	9.39E+03	7.68E+03	1.00E+04
10	1.83E+03	2.27E+03	1.66E+03	2.09E+03
15	5.78E+02	7.11E+02	4.93E+02	6.10E+02
20	2.23E+02	2.68E+02	1.83E+02	2.25E+02
25	9.86E+01	1.17E+02	7.98E+01	9.75E+01
30	4.84E+01	5.63E+01	3.89E+01	4.72E+01
40	1.44E+01	1.65E+01	1.23E+01	1.38E+01
50	5.28E+00	6.04E+00	4.48E+00	4.87E+00
59	2.23E+00	2.49E+00	2.04E+00	2.27E+00

Table 3: Mass dependence of the integrated bottom quark p_t distribution at 1.8 TeV. MRSD0 parton distributions, $\mu_F = \mu_0/4$, $\Lambda_0 = 215$ MeV, $\Lambda_+ = 275$ MeV.

p_t^{min} (GeV)	Λ_0		Λ_+	
	$m_b=4.5$ GeV	$m_b=4.75$ GeV	$m_b=4.5$ GeV	$m_b=4.75$ GeV
0	2.6E+04	2.2E+04	3.8E+04	3.0E+04
5	8.0E+03	7.2E+03	1.0E+04	9.4E+03
10	1.9E+03	1.8E+03	2.4E+03	2.3E+03
20	2.3E+02	2.2E+02	2.8E+02	2.7E+02

Table 4: Integrated ψ p_t distribution from B decays, from charmonium production ($\chi + \psi$) and relative B fraction at 1.8 TeV. MRSD0, $\Lambda_0 = 215$ MeV, $\Lambda_+ = 275$ MeV. BR($J/\psi \rightarrow \mu^+ \mu^-$) included.

$p_t^{min,\psi}$ (GeV)	$\Lambda_0, \mu_F = \mu_0$			$\Lambda_+, \mu_F = \mu_0/4$		
	$\sigma_B \cdot$ BR (nb)	$\sigma_\chi \cdot$ BR (nb)	f_B (%)	$\sigma_B \cdot$ BR (nb)	$\sigma_\chi \cdot$ BR (nb)	f_B (%)
3	2.6E+00	5.4E+00	32	5.4E+00	3.9E+01	12
4	1.7E+00	1.9E+00	46	3.4E+00	1.5E+01	19
5	1.1E+00	7.6E-01	58	2.2E+00	6.0E+00	26
6	6.7E-01	3.4E-01	66	1.4E+00	2.8E+00	33
8	2.9E-01	8.7E-02	77	6.3E-01	7.7E-01	45
10	1.4E-01	2.9E-02	83	3.2E-01	2.6E-01	55
12	7.8E-02	1.2E-02	86	1.7E-01	1.0E-01	62
14	4.4E-02	4.9E-03	89	1.0E-01	5.0E-02	67
16	2.6E-02	2.5E-03	91	6.1E-02	2.5E-02	71
18	1.7E-02	1.3E-03	92	3.9E-02	1.3E-02	75
20	1.1E-02	7.3E-04	93	2.5E-02	6.9E-03	78
25	4.2E-03	1.9E-04	95	9.4E-03	1.9E-03	82
30	1.9E-03	4.9E-05	97	4.1E-03	5.2E-04	88

Table 5: CDF Mass Measurements Compared with World Values

Decay Mode	PDG Mass (MeV)	SVX Mass
$\Lambda \rightarrow p\pi$	1115.63 ± 0.05	1115.6 ± 0.2
$J/\psi \rightarrow \mu\mu$	3096.93 ± 0.09	3096.1 ± 0.2
$\psi(2S) \rightarrow J/\psi\pi\pi$	3686.00 ± 0.10	$3686. \pm 1.$
$B_u \rightarrow J/\psi K^\pm$	5278.6 ± 2.0	$5277. \pm 3.$
$B_d \rightarrow J/\psi K^{0*}$	5278.7 ± 2.1	$5277. \pm 4.$

Table 6: Values of some parameters of interest for the decay of the B_c . The expectations of different models (QCD sum rules (SR) or potential models (PM)), together with uncertainty estimates, are included whenever available. (ISGW, see [39], BSW, see [40]).

Lifetime	$0.5 \div 1.5 \times 10^{-12} \text{ sec (PM) , } 0.9 \times 10^{-12} \text{ sec (SR)}$
f_{B_c}	$550 \pm 50 \text{ MeV (PM) , } 360 \pm 60 \text{ MeV (SR)}$
$\text{BR}(B_c \rightarrow \psi + X)$	$24 \pm 10\% \text{ (PM)}$
$\text{BR}(B_c \rightarrow \psi l \nu)$	$3 \pm 1\% \text{ (ISGW,BSW) , } 0.8\% \text{ (SR)}$
$\text{BR}(B_c \rightarrow \psi l \nu + X)$	$4.7\% \text{ (ISGW,BSW)}$
$\text{BR}(B_c \rightarrow \psi \pi)$	$0.2\% \text{ (ISGW,BSW)}$

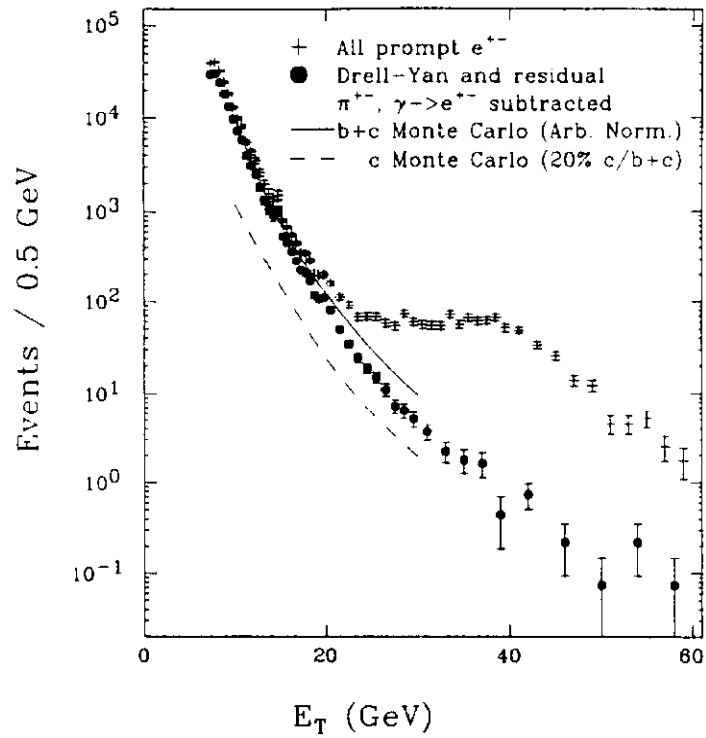


Figure 1: The p_T spectrum of electron candidates.

Electrons

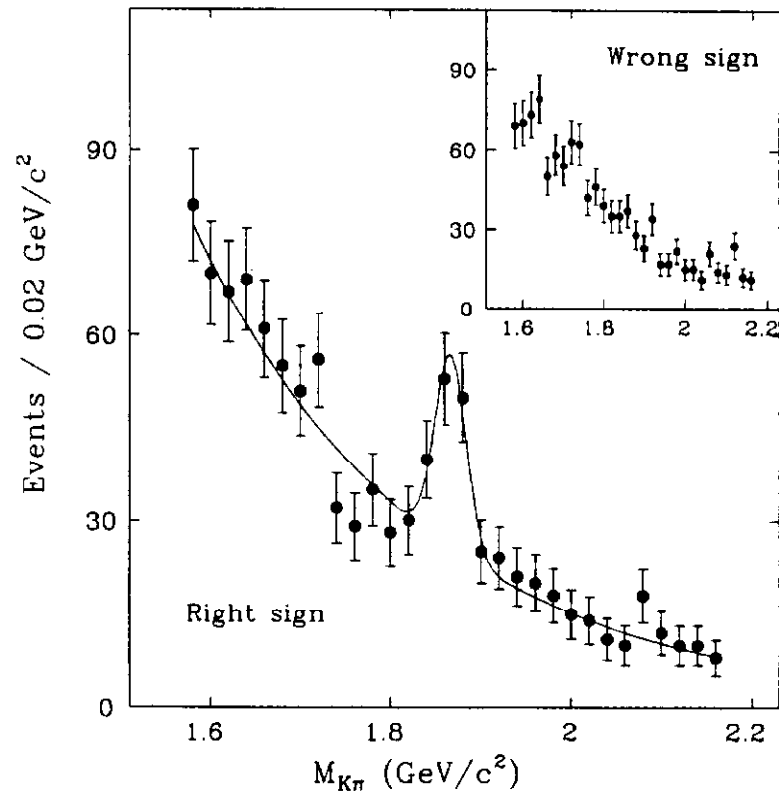


Figure 2: Right sign $K^- \pi^+$ invariant mass distribution in the electron events.

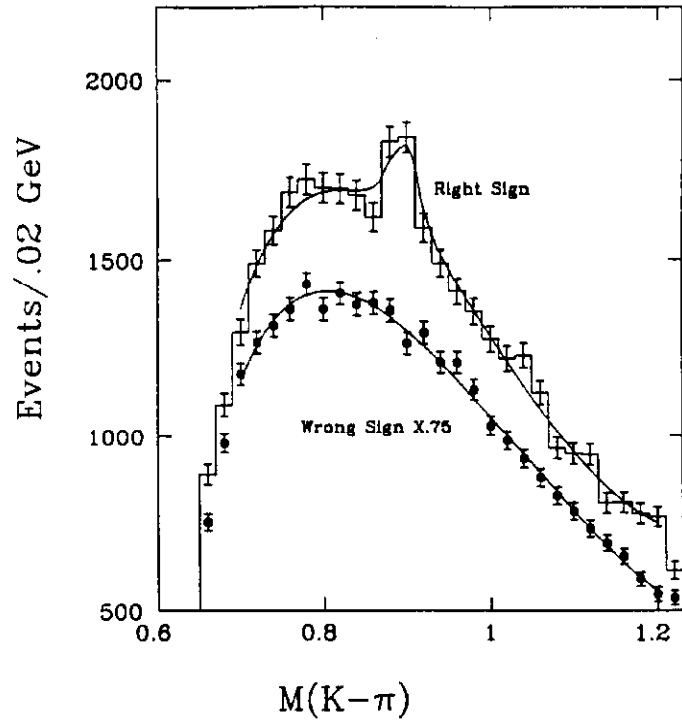


Figure 3: $K\pi$ mass spectra in the $K^*(890)$ region for 'right-sign' combinations to come from b decay ($e^- \bar{K}^{*0}$) and for 'wrong-sign' combinations ($e^- K^{*0}$), scaled by 0.75.

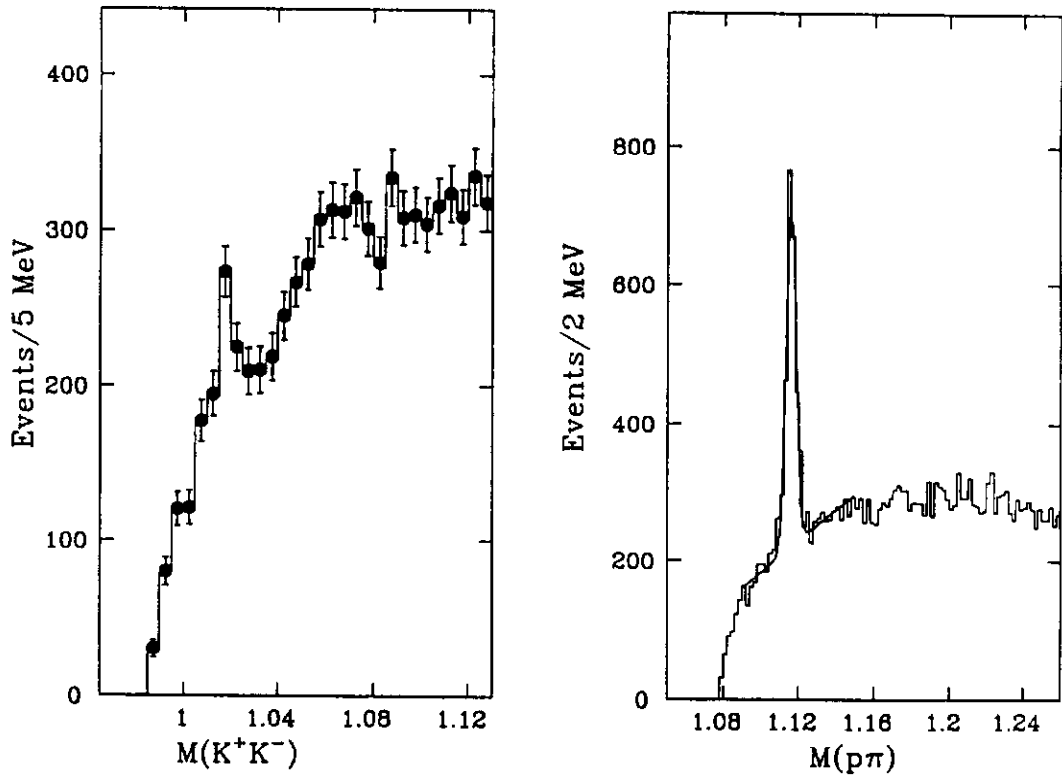


Figure 4: Signals for $\Lambda \rightarrow p\pi$ (right) and $\phi \rightarrow KK$ (left) in the electron trigger sample.

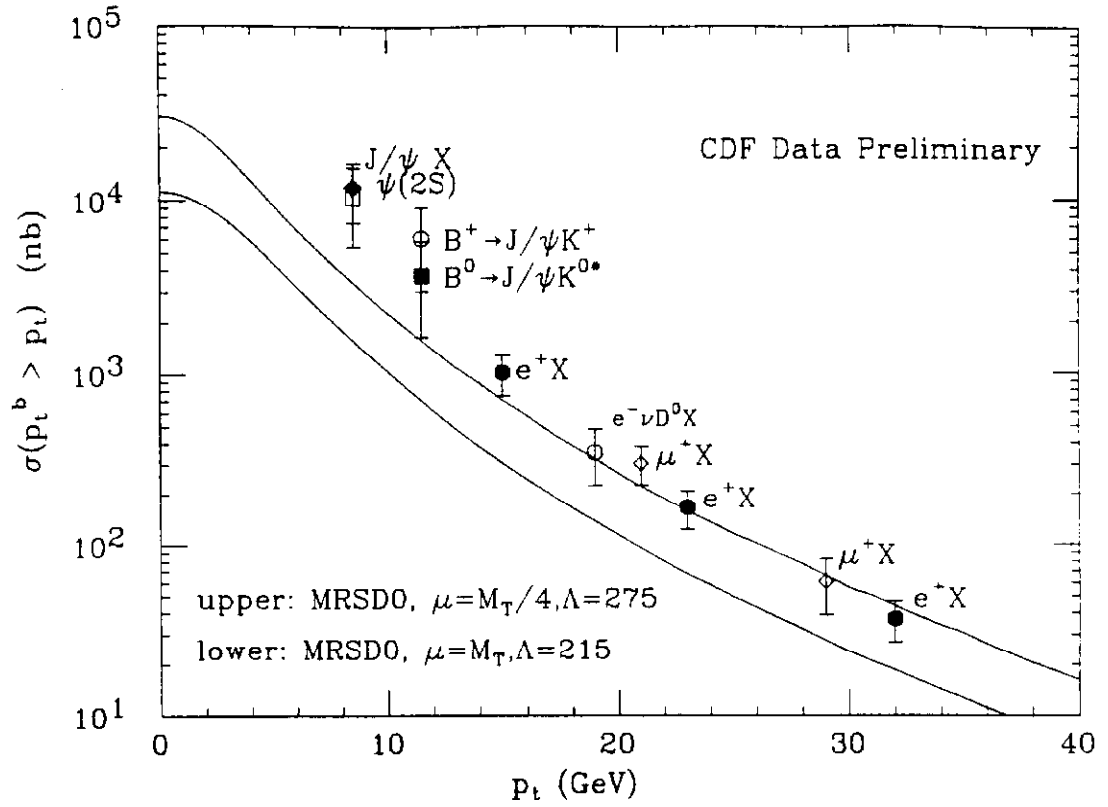


Figure 5: Integrated $b p_t$ distribution at 1.8 TeV: CDF data versus NLO QCD. The J/ψ point assumes a B fraction in the inclusive J/ψ sample of $63 \pm 17\%$.

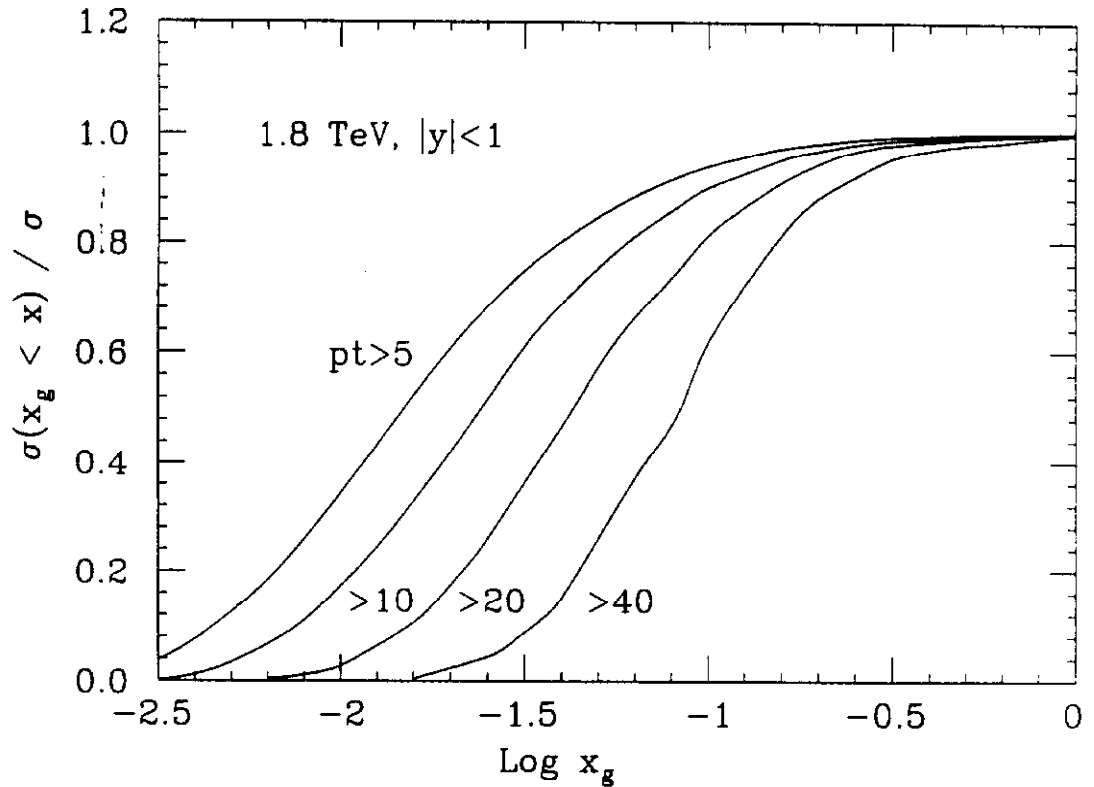


Figure 6: Fraction of the NLO QCD b cross section at 1.8 TeV coming from gluons with $x_g < x$, for different p_t thresholds.

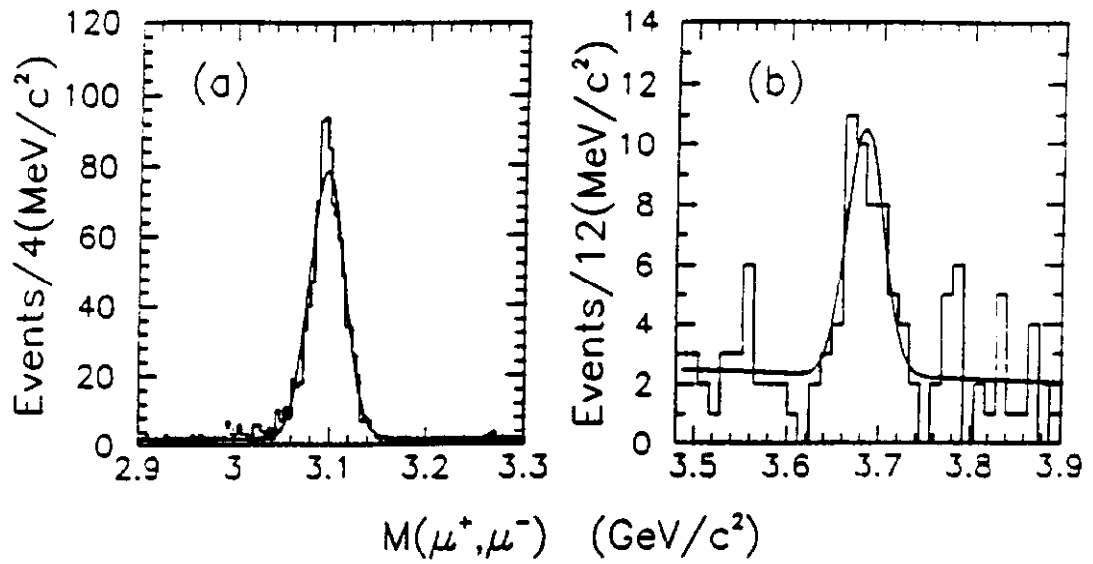


Figure 7: J/ψ and ψ' mass spectra in the dimuon channel from the 1988/89 run.

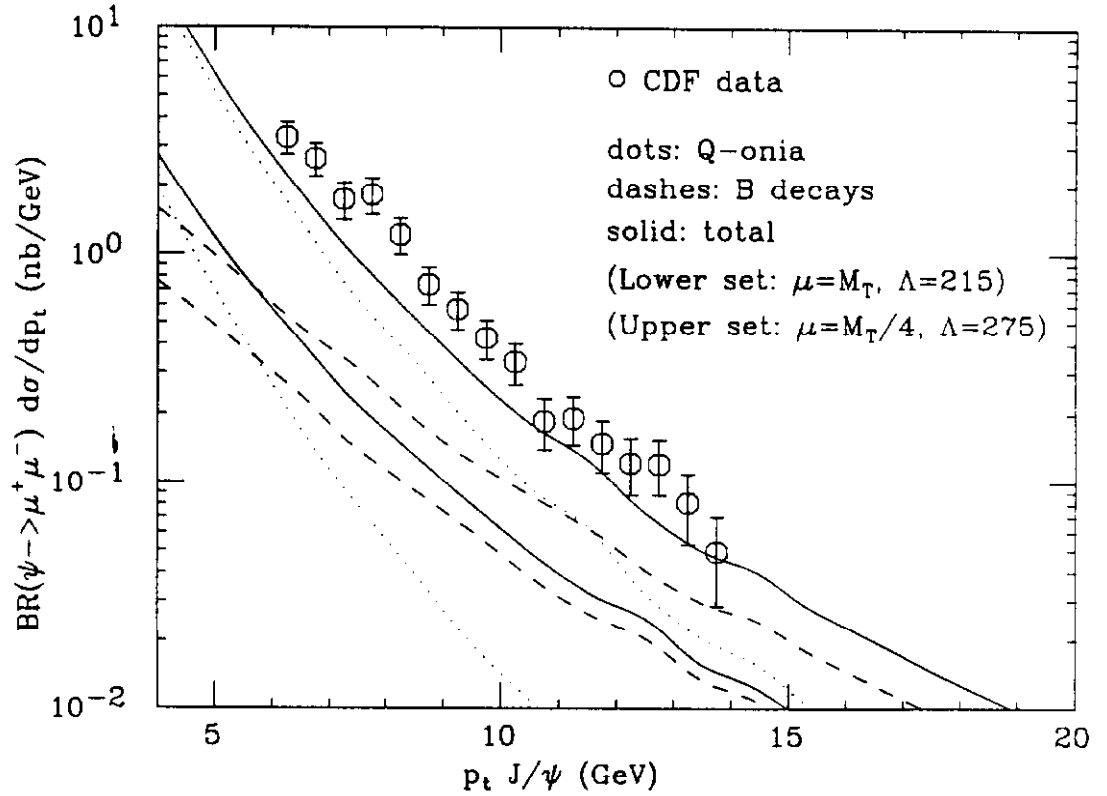


Figure 8: Differential J/ψ p_t distribution at 1.8 TeV: CDF data versus different QCD contributions, as shown in the legend.

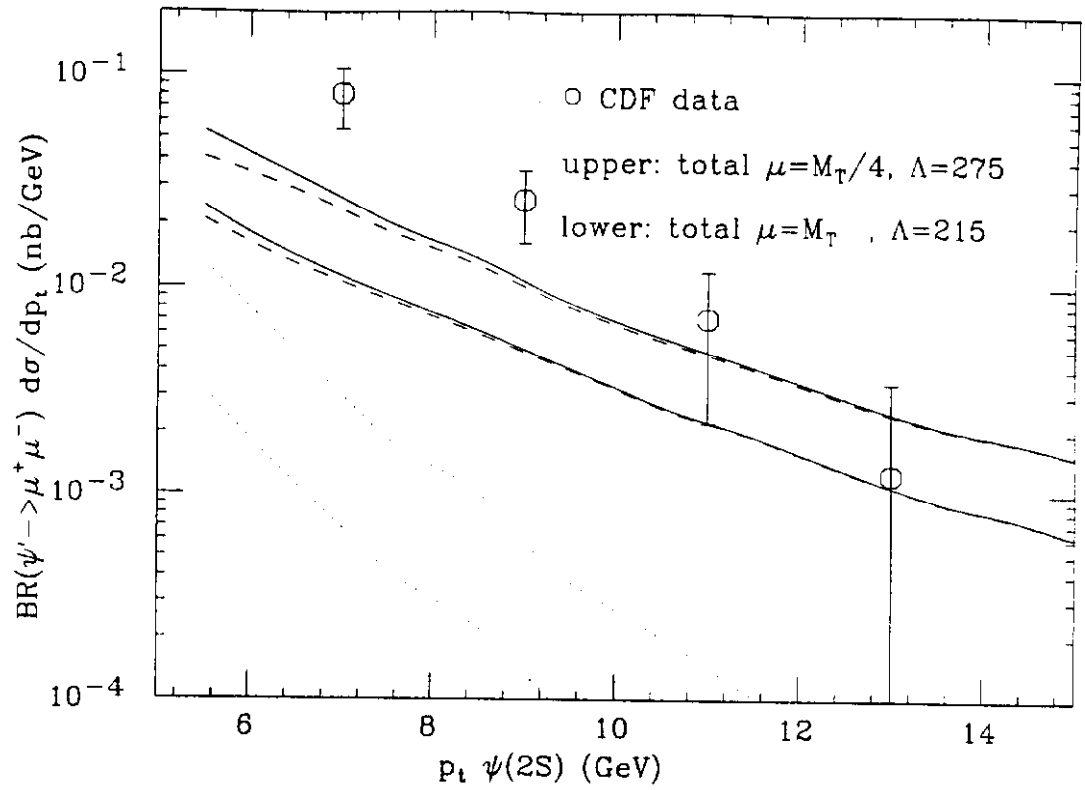


Figure 9: Differential $\psi(2S)$ p_t distribution at 1.8 TeV: CDF data versus total QCD. The different contributions from direct production and B decays are labeled as in the previous Figure.

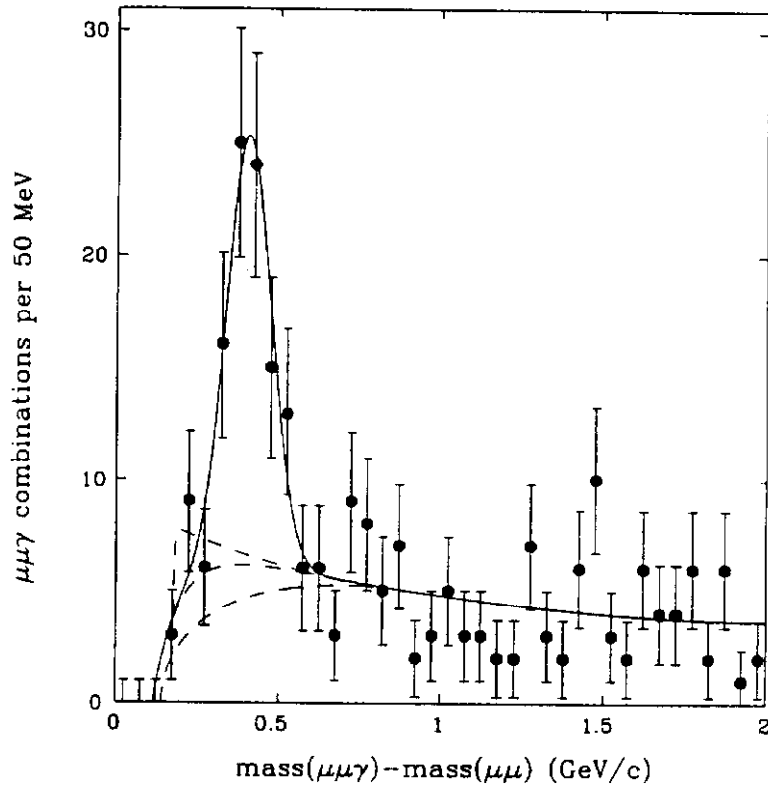


Figure 10: χ signal in the inclusive J/ψ sample.

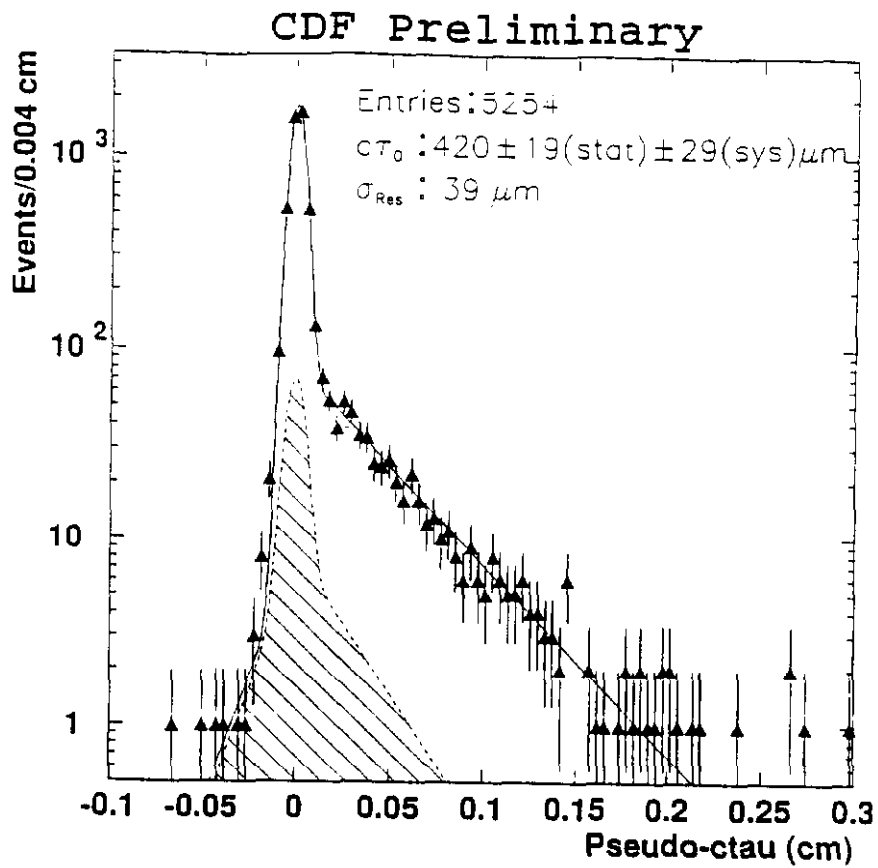


Figure 11: Distribution of the corrected proper transverse decay length of J/ψ mesons.

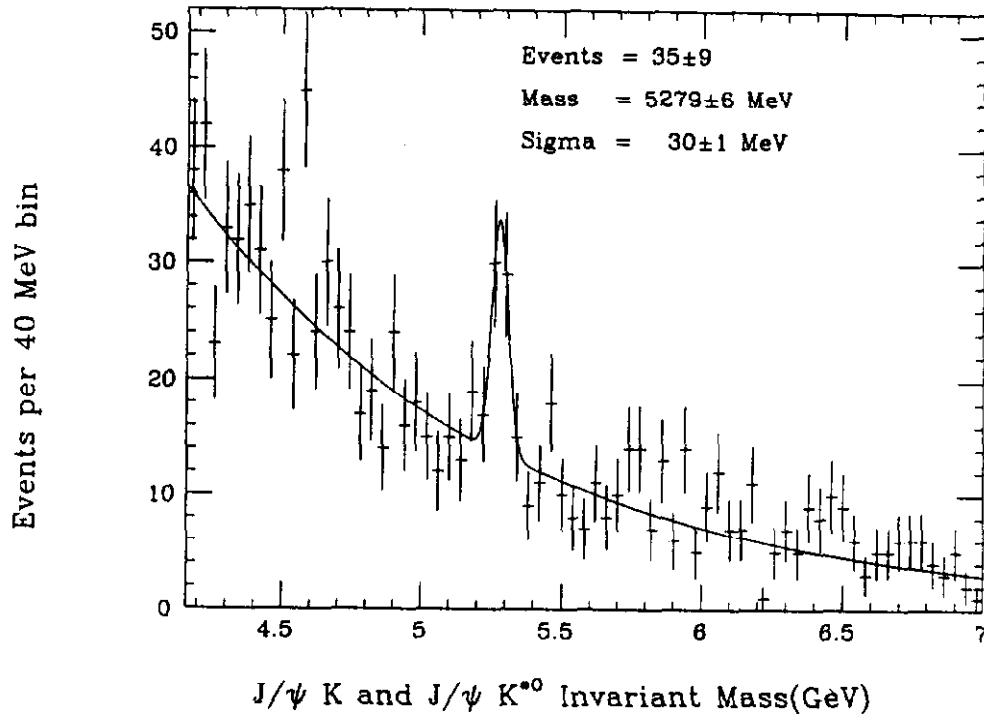


Figure 12: $B^\pm \rightarrow J/\psi K^\pm$ and $B^0 \rightarrow J/\psi K^*0$ mass spectra from the 1988/89 run.

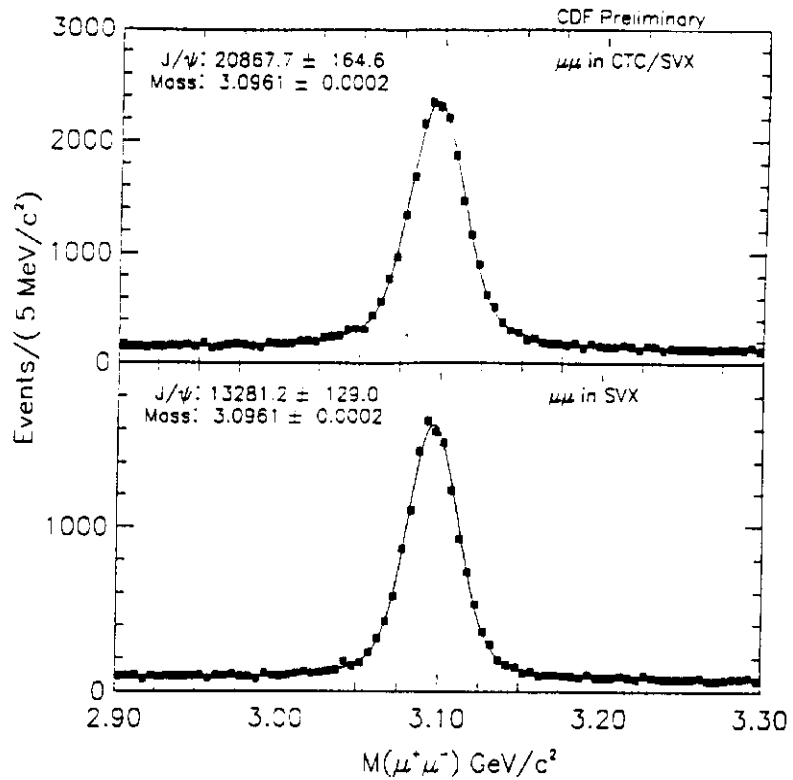


Figure 13: Preliminary J/ψ mass spectra from the 1992/93 run.

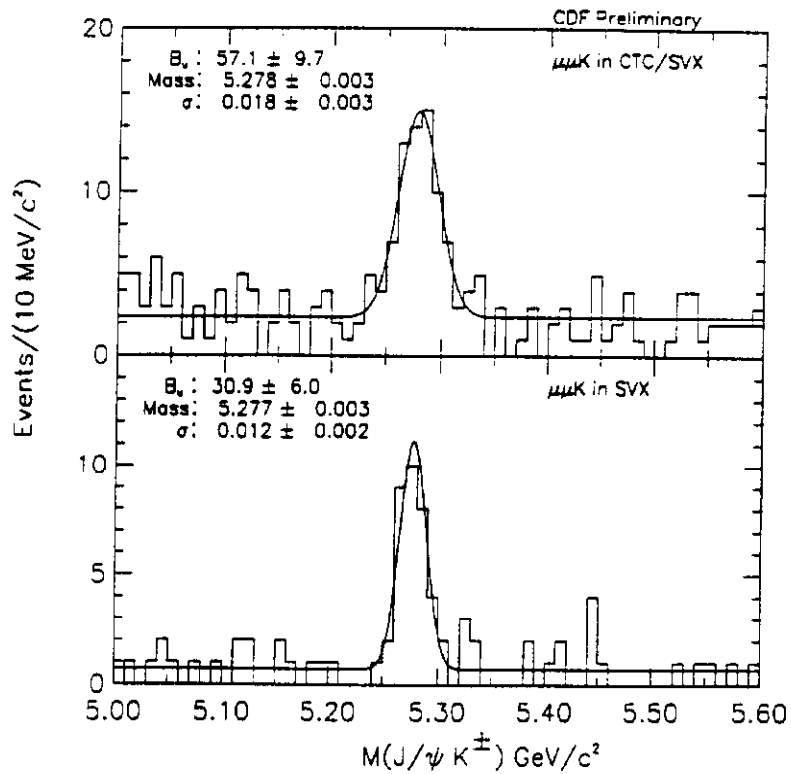


Figure 14: Preliminary $B^\pm \rightarrow J/\psi K^\pm$ mass spectra from the 1992/93 run. The upper plot is from events with tracks in the CTC/SVX, the lower plot from events with all relevant tracks in the SVX.

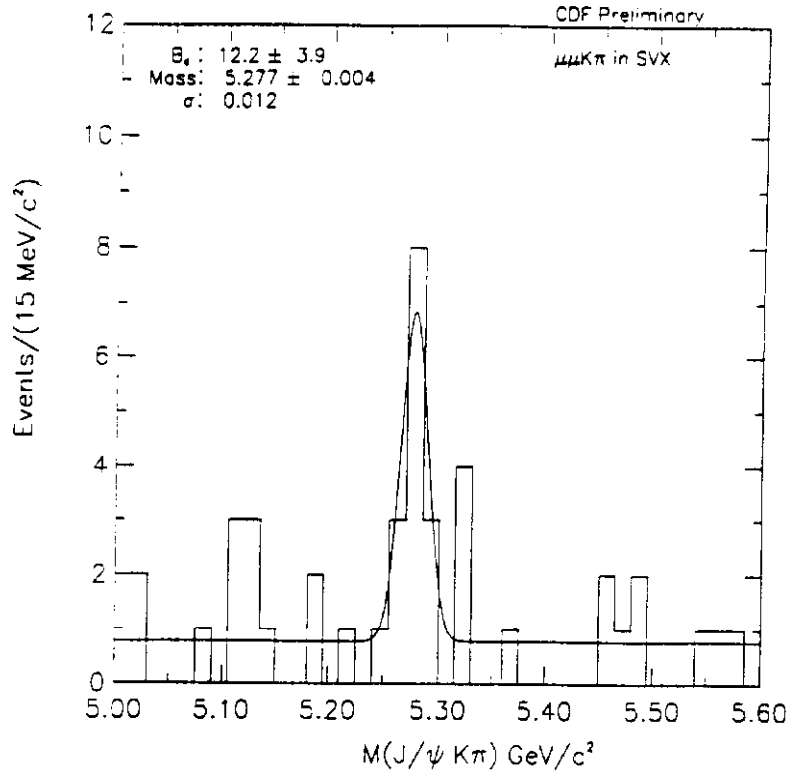


Figure 15: Preliminary $B^\pm \rightarrow J/\psi K^*$ mass spectra from the 1992/93 run.

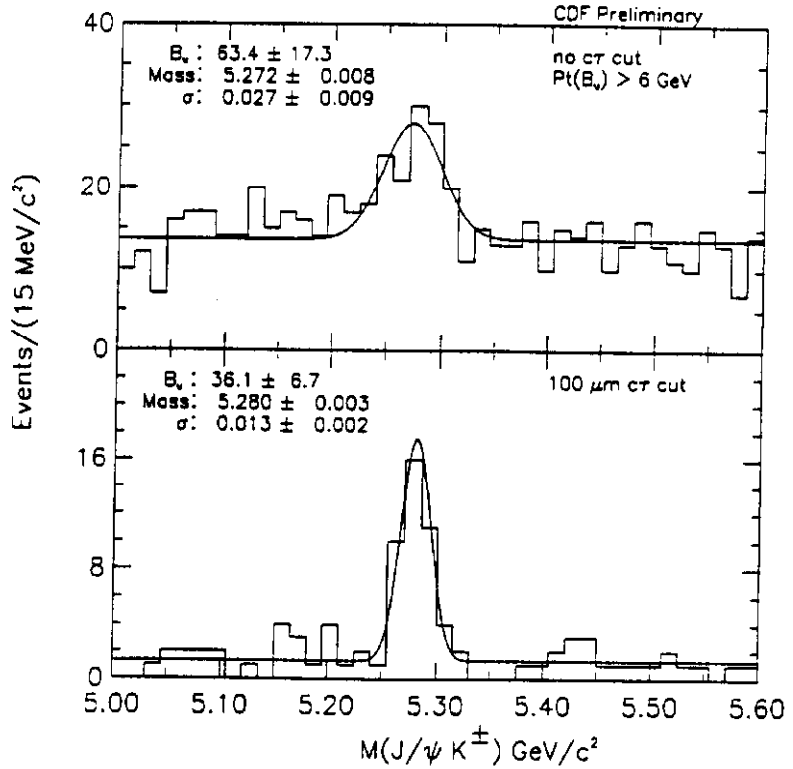


Figure 16: Preliminary $B^\pm \rightarrow J/\psi K^\pm$ mass spectra from the 1992/93 run. Here $p_t(K) > 6 \text{ GeV}$. The upper plot is from events with tracks in the CTC/SVX and no cr cut. The lower plot from events with all relevant tracks in the SVX and $cr > 100 \mu\text{m}$.

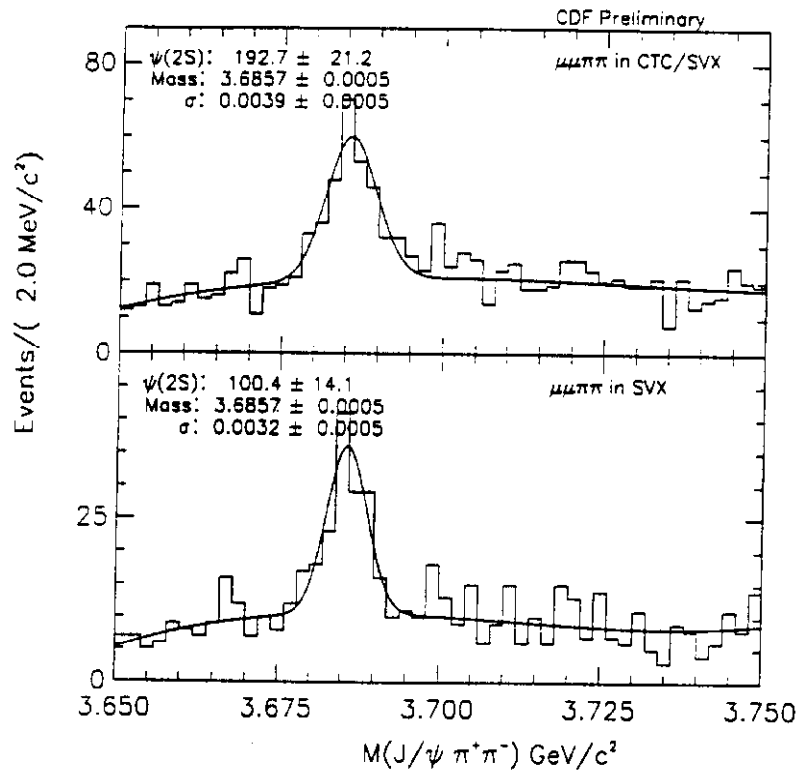


Figure 17: Preliminary $J/\psi\pi\pi$ mass spectrum from the 1992/93 data.